SID 61-459

SATELLITE RENDEZVOUS STUDY

SECOND QUARTERLY REPORT

(31 August, 1961 through 30 November)

15 December 1961

Prepared by

Paul R. DesJardins

and

David F. Bender

Space Sciences Laboratory

Approved by

E R van Driest

E. R. van Driest
Director

NORTH AMERICAN AVIATION, INC.
SPACE and INFORMATION SYSTEMS DIVISION

CONTENTS

I. INTRODUCTION

This report concerns effort expended on the Satellite Rendezvous Study Contract (NAS 8-1582) which is a continuation of the original Analytical Study of Satellite Rendezvous (Contract DA-04-495-ORD-1690) described in Reference 1. The present study is being conducted at the Space Sciences Laboratory of the Space and Information Systems Division of North American Aviation, Inc. This report covers the period 31 August through 30 November 1961.

During this period work has been done in two areas: (A) The time to transfer and its dependence on the three parameters of the two-impulse transfer case has been included in the computing programs, and (B) The technique of representing the impulse surface by three dimension quadratic surfaces has been further tested. In connection with this work, schemes for orbit projections as presentations on an oscilloscope have developed.

In addition a paper "Co-planar Two-Impulse Orbital Transfers" was presented at the ARS Space Flight Report to the Nation, in October 1961. Copies of the preprint (ARS preprint 2063-61) are included. A second paper, entitled "Optimum Co-planar Two-Impulse Transfers between Elliptic Orbits" has been written and accepted by the I.A.S. for presentation at the annual meeting in New York, January 24-27, 1962. Copies of this preprint are not yet available. They will be attached to the next quarterly report.

The notation used is the same as that of previous reports. Figure A1, Transfer Geometry and the notation list are essentially copies from previous reports.

Reference 1: Kerfoot, H. P., D. F. Bender and P. R. DesJardins, "Analytical Study of Satellite Rendezvous," North American Aviation, Inc., Space & Information Systems Division, Report No. MD 59-272, 20 October 1960.

II. TECHNICAL NOTES

(A) The Time Constraint for Two-Impulse Transfer

The relative positions of the ferry on the initial orbit and the target satellite on the final orbit must be included in the rendezvous problem. Let τ be the time interval between the passage of ferry and of the target satellite across the ascending node N (see Fig. A1), and consider the requirement to effect rendezvous in the ensuing revolution of the target. The traverse times t_1, t, and t_2 are associated with the true anomaly intervals ϕ_1, $\Delta\theta$, and ϕ_2 respectively. The condition on these time intervals for rendezvous is $\tau + t_2 = t_1 + t$. It can be written as:

$$\tau = t_1 + t - t_2. \qquad \text{(A1)}$$

If one waits for the other nodal passages of the ferry or of the target, the time interval τ will change by amounts that are obtained from integral multiples of the periods. Thus for any given orbit pair and initial satellite conditions a series of values of τ will occur. If ranges of τ acceptable for transfer can be established, then orbital transfer might be effected by waiting until τ assumes a satisfactory value. If this is impractical a phase change maneuver on one of three orbits involved could be used, with of course, the expenditure of impulse.

Because Eq. (A1) the time interval, τ , for rendezvous can be considered a function of the three parameters ϕ_1, ϕ_2 and ϕ_3 of the two-impulse problem. The procedure for optimizing the impulse for a given value of τ consists in finding points in ϕ space where the surfaces I = constant and τ = constant are parallel. This type of optima will be called constrained optima.

Suppose that for some value of τ a transfer has been found and it is desired to optimize the impulse. We want to move in ϕ space over the surface τ = constant in the direction of the component of -grad I. Let $\bar{S}$ be the unit vector in the direction of grad τ . The desired direction is:

$$\bar{P} \equiv - \left[\text{grad } I - (\bar{S} \cdot \text{grad } I)\, \bar{S} \right] \qquad \text{(A2)}$$

Thus it is necessary to obtain the derivatives of τ with respect to the parameters ϕ_1, ϕ_2, ϕ_3. Fortunately these derivatives

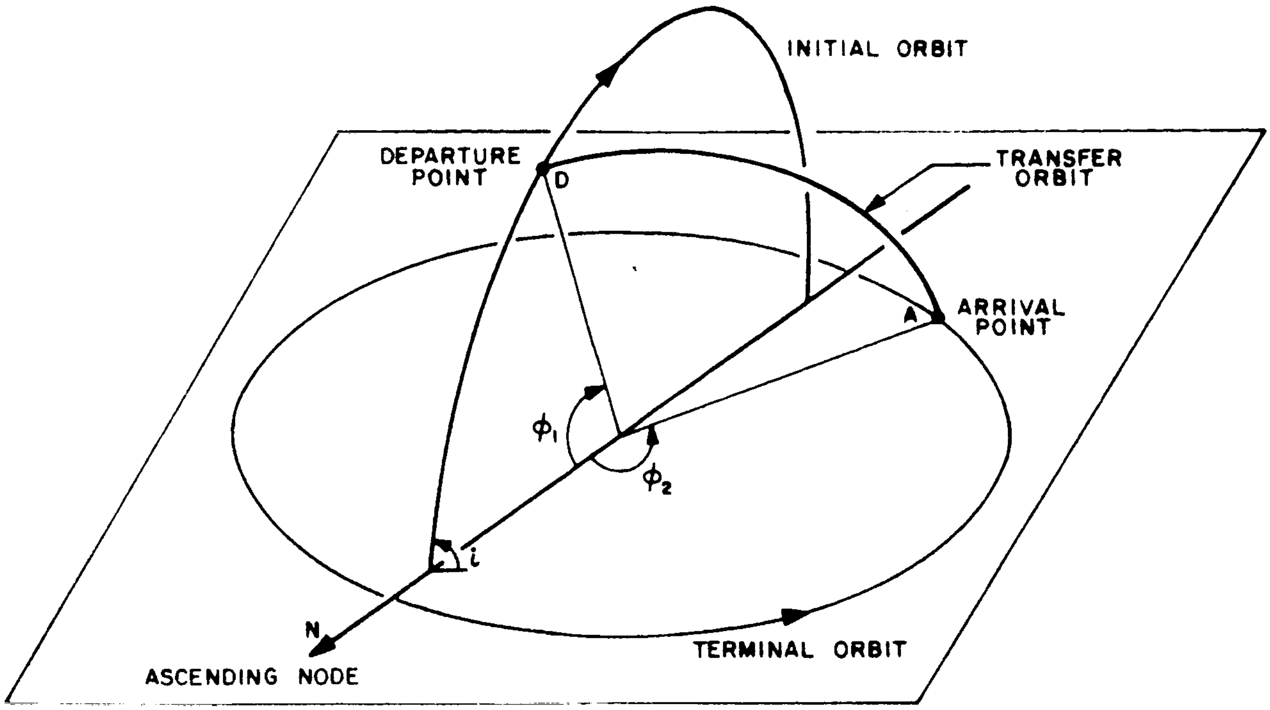

PROJECTION ON UNIT SPHERE

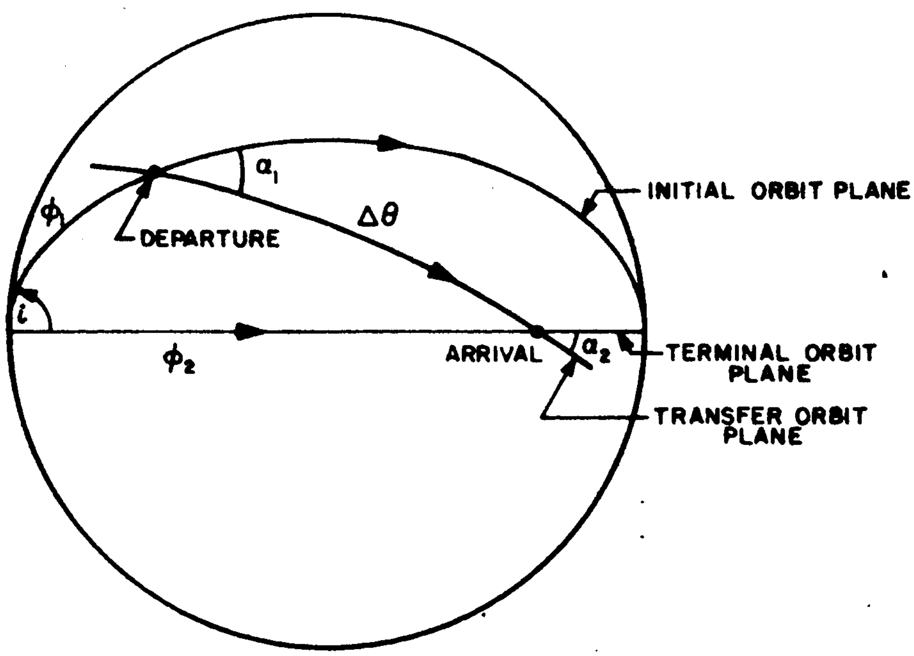

FIG. A1 TRANSFER GEOMETRY

are easily obtainable, as explained in the following series of equations and comments.

$$\frac{\partial \tau}{\partial \phi_1} = \frac{\partial t_1}{\partial \phi_1} + \frac{\partial t}{\partial \phi_1} \qquad (A3)$$

$$\frac{\partial \tau}{\partial \phi_2} = \frac{\partial t}{\partial \phi_2} - \frac{\partial t_2}{\partial \phi_2} \qquad (A4)$$

$$\frac{\partial \tau}{\partial \phi_3} = \frac{\partial t}{\partial \phi} \qquad (A5)$$

$$\frac{\partial t_1}{\partial \phi_1} = \frac{r_1^2}{\sqrt{\mu p_1}} \quad \text{and} \quad \frac{\partial t_2}{\partial \phi_2} = \frac{r_2^2}{\sqrt{\mu p_2}} \quad \text{(conservation of angular momentum)} \qquad (A6,\ A7)$$

$$t = \frac{1}{n}\left[E_2 - E_1 - e\,(\sin E_2 - \sin E_1)\right] \qquad (A8)$$

where E_1 and E_2 are the eccentric anomalies of D and A on the transfer orbit.

$$\frac{\partial t}{\partial \phi_i} = \frac{3}{2}\,\frac{t}{a}\,\frac{\partial a}{\partial \phi_i} + \frac{1}{n}\left[\frac{r_2}{p}\,(1-e^2)\,\frac{\partial E_2}{\partial \phi_i} - \frac{r_1}{p}\,(1-e^2)\,\frac{\partial E_1}{\partial \phi_i} - (\sin E_2 - \sin E_1)\,\frac{\partial e}{\partial \phi_i}\right] \qquad (A9)$$

$$i = 1,\ 2,\ 3$$

To obtain $\frac{\partial a}{\partial \phi_i}$ write

$$r_2 = \frac{p_2}{1+e_2 \cos(\phi_2 - \omega_2)} = \frac{a(1-e^2)}{1+e \cos \phi_3} \qquad (A10)$$

The results are:

$$\frac{1}{a}\frac{\partial a}{\partial \phi_1} = \left[\frac{1+e^2}{1-e^2} - \frac{r_2}{p}\right]\frac{1}{e}\frac{\partial e}{\partial \phi_1} \qquad \text{(A11)}$$

$$\frac{1}{a}\frac{\partial a}{\partial \phi_2} = \left[\frac{1+e^2}{1-e^2} - \frac{r_2}{p}\right]\frac{1}{e}\frac{\partial e}{\partial \phi_2} + \frac{e_2\, r_2}{p_2}\sin(\phi_2 - \omega_2) \qquad \text{(A12)}$$

$$\frac{1}{a}\frac{\partial a}{\partial \phi_3} = \left[\frac{1+e^2}{1-e^2} - \frac{r_2}{p}\right]\frac{1}{e}\frac{\partial e}{\partial \phi_3} - \frac{e r_2}{p}\sin \phi_3 \qquad \text{(A13)}$$

To obtain $\dfrac{\partial E_{1,2}}{\partial \phi_i}$ use

$$\cos E_1 - \cos(\phi_3 - \Delta\theta) = e\left[1 - \cos E_1 \cos(\phi_3 - \Delta\theta)\right] \qquad \text{(A14)}$$

and

$$\cos E_2 - \cos \phi_3 = e\left[1 - \cos E_2 \cos \phi_3\right] \qquad \text{(A15)}$$

The results are:

$$\frac{\partial E_1}{\partial \phi_1} = -\frac{\sin E_1}{1-e^2}\frac{\partial e}{\partial \phi_1} - \frac{\sin E_1}{\sin(\phi_3 - \Delta\theta)}\frac{\partial \Delta\theta}{\partial \phi_1} \qquad \text{(A16)}$$

$$\frac{\partial E_1}{\partial \phi_2} = -\frac{\sin E_1}{1-e^2}\frac{\partial e}{\partial \phi_2} - \frac{\sin E_1}{\sin(\phi_3 - \Delta\theta)}\frac{\partial \Delta\theta}{\partial \phi_2} \qquad \text{(A17)}$$

$$\frac{\partial E_1}{\partial \phi_3} = -\frac{\sin E_1}{1-e^2}\frac{\partial e}{\partial \phi_3} + \frac{\sin E_1}{\sin(\phi_3 - \Delta\theta)} \qquad \text{(A18)}$$

$$\frac{\partial E_2}{\partial \phi_1} = -\frac{\sin E_2}{1-e^2}\frac{\partial e}{\partial \phi_1} \qquad \text{(A19)}$$

$$\frac{\partial E_2}{\partial \phi_2} = - \frac{\sin E_2}{1-e^2} \frac{\partial e}{\partial \phi_2} \tag{A20}$$

$$\frac{\partial E_2}{\partial \phi_3} = - \frac{\sin E_2}{1-e^2} \frac{\partial e}{\partial \phi_3} + \frac{\sin E_2}{\sin \phi_3} \quad . \tag{A21}$$

Since

$$\cos \Delta\theta = \cos \phi_1 \cos \phi_2 + \sin \phi_1 \sin \phi_2 \cos i_1 \quad , \tag{A22}$$

$$\frac{\partial \Delta\theta}{\partial \phi_1} = \frac{\sin(\phi_1 - \phi_2) + \cos \phi_1 \sin \phi_2 (1 - \cos i_1)}{\sin \Delta\theta} \tag{A23}$$

$$\frac{\partial \Delta\theta}{\partial \phi_2} = \frac{\sin(\phi_2 - \phi_1) + \cos \phi_2 \sin \phi_1 (1 - \cos i_1)}{\sin \Delta\theta} \quad . \tag{A24}$$

Finally to find $\frac{\partial e}{\partial \phi_i}$ use

$$\frac{r_1}{r_2} = \frac{p_1}{p_2} \frac{(1 + e_2 \cos (\phi_2 - \omega_2)}{1 + e_1 \cos (\phi_1 - \omega_1)} = \frac{1 + e \cos \phi_3}{1 + e \cos (\phi_3 - \Delta\theta)} \quad . \tag{A25}$$

The results are:

$$\frac{\partial e}{\partial \phi_1} = \frac{e}{r_1 - r_2} \left[\frac{e_1 r_1 p}{p_1} \sin (\phi_1 - \omega_1) + e r_1 \sin (\phi_3 - \Delta\theta) \frac{\partial \Delta\theta}{\partial \phi_1} \right] \tag{A26}$$

$$\frac{\partial e}{\partial \phi_2} = \frac{e}{r_1 - r_2} \left[- \frac{e_2 r_2 p}{p_2} \sin (\phi_2 - \omega_2) + e r_1 \sin (\phi_3 - \Delta\theta) \frac{\partial \Delta\theta}{\partial \phi_2} \right] \tag{A27}$$

$$\frac{\partial e}{\partial \phi_3} = \frac{e^2}{r_1 - r_2} \left[r_2 \sin \phi_3 - r_1 \sin (\phi_3 - \Delta\theta) \right] \qquad (A28)$$

Using these equations the computation of grad τ has been added to that part of the 7090 program where grad I is computed for any orbit pair and ϕ_1, ϕ_2, ϕ_3.

In order to find constrained optima the following procedure has been tried. First the optimum transfer was selected, point A in Fig. A2. Next the points B and B' are chosen each lying 1° (an arbitrary choice) away from A along grad τ at A. Then a series of points $C_1, C_2, \ldots$ were chosen lying along the direction given by Equation A2 from B, $C_1 \ldots$ respectively. Results are shown in Tables A1 and A2 for two orbit pairs. Table A3 shows the approach to a constrained optimum starting from a point that was arbitrarily selected near the optimum for the case given in Table A2.

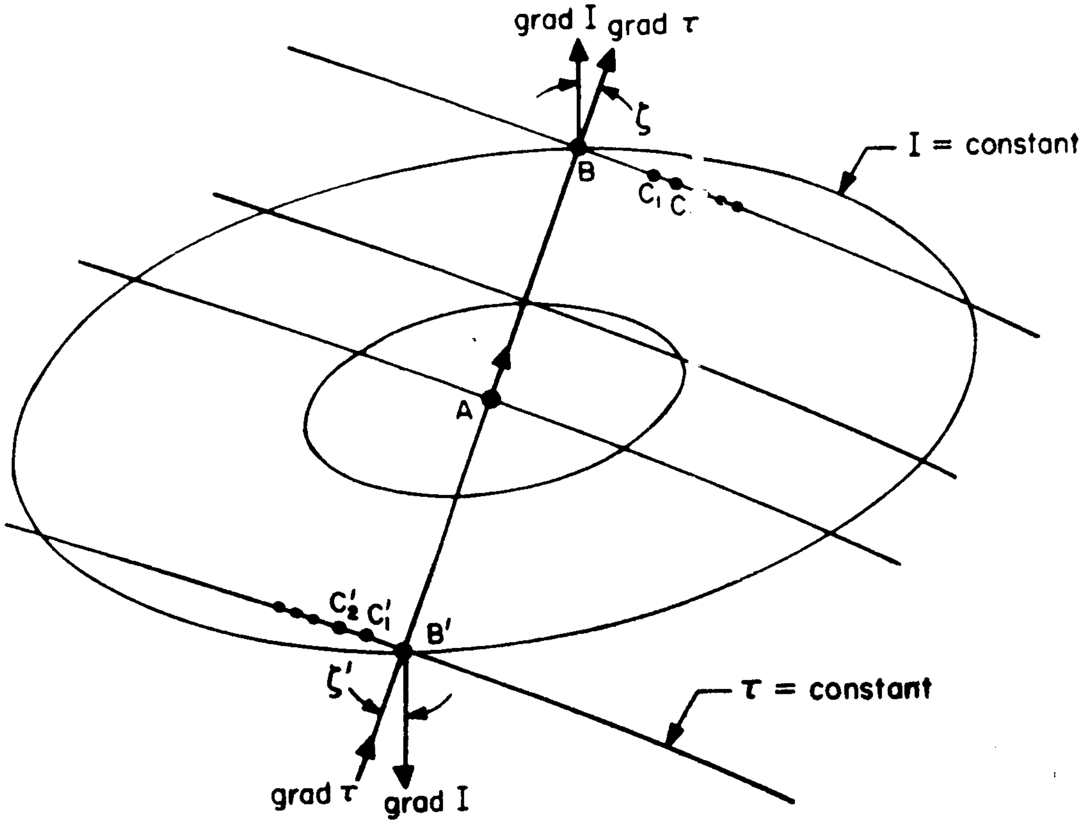

FIG. A2 GEOMETRY FOR LOCATING CONSTRAINED OPTIMA

TABLE A1. APPROACH TO CONSTRAINED OPTIMA

Point (See Fig. A2)	Total Impulse	Time Difference (τ)	Angle between grad I and grad τ
A (optimum)	4902.[illegible] ft/sec	[illegible]2.410 sec	
B (AB = +1°)	4904.[illegible]4	871.112	22°.2[illegible]
C_1 (BC_1 = .5°)	4903.98	[illegible]1.124	1[illegible]°.43
C_2 (C_1C_2 = .5°)	4903.5[illegible]	[illegible]	12°.3[illegible]
C_3 (C_2C_3 = .5°)	4903.[illegible]4	[illegible]	1°.2[illegible]
B' (AB' = -1°)	4904.[illegible]4	[illegible]3.4[illegible]	1[illegible]0° - 20°.23
C_1' ($B'C_1'$ = .5°)	4904.02	[illegible]3.41[illegible]	1[illegible]0° - 1[illegible]°.[illegible]3
C_2' ($C_1'C_2'$ = .5°)	4903.[illegible]	[illegible]3.43[illegible]	1[illegible]0° - 11°.41
C_3' ($C_2'C_3$ = .5°)	4903.51	[illegible]3.422	1[illegible]0° - 1°.89

Orbit Geometry

p_1 = 5000 mi $\quad e_1$ = .20 $\quad \omega_1$ = -[illegible]° $\quad i_1$ = 5°

p_2 = 6000 mi $\quad e_2$ = .20 $\quad \omega_2$ = 30°

For A $\quad \phi_1$ = 73°.82 $\quad \phi_2$ = 1[illegible]°.5[illegible] $\quad \phi_3$ = 1[illegible]°.[illegible] $\quad \Delta\theta$ = 113°.[illegible]1

For C_3 $\quad \phi_1$ = 73°.63 $\quad \phi_2$ = 187°.79 $\quad \phi_3$ = 1[illegible]0°.52 $\quad \Delta\theta$ = 114°.12

A2. APPROACH TO CONSTRAINED OPTIMUM

Point (See Fig. A2)	Total Impulse	Time Difference (τ)	Angle between [illegible] and [illegible] τ
A optimum	5[illegible].[illegible]3 ft/sec	-[illegible]02.04 sec	
B (AB = 1^{o})	5[illegible]45.36	-[illegible]	2^{o}.[illegible]3
C_1 (BC_1 = .[illegible]2^{o})	[illegible]443.[illegible]	-[illegible]	1^{o}.[illegible]1
C_2 (C_1C_2 = .34^{o})	5[illegible]42.[illegible]5	-[illegible]	1^{o}.[illegible]
C_3 (C_2C_3 = .$2[illegible]^{o}$)	5[illegible]42.50	-[illegible]	1^{o}.39

Orbit Geometry

p_1 = 5000 mi $\qquad e_1$ = .2 $\qquad \omega_1 = -[illegible]$ $\qquad i_1 = 15^{o}$

p_2 = 6000 mi $\qquad e_2$ = .2 $\qquad \omega_2 = -[illegible]$

For A $\quad \theta_1 = 14^{o}.42 \qquad \theta_2 = 1[illegible]^{o}.[illegible]2 \qquad \theta_3 = 23[illegible]^{o}.20 \qquad \Delta\theta = 1[illegible]^{o}.55$

For C_3 $\quad \theta_1 = 13^{o}.38 \qquad \theta_2 = 1[illegible]3^{o}.2[illegible] \qquad \theta_3 = 240^{o}.0[illegible] \qquad \Delta\theta = 160^{o}.04$

TABLE A3. APPROACH TO CONSTRAINED OPTIMUM

Point	Total Impulse	Time Difference (τ)	Angle between [illegible] and [illegible] τ
C_1 (not optimum)	5[illegible]12.73 ft/sec	-1[illegible].2[illegible] sec	1[illegible]0°-2[illegible]
C_2 (C_1C_2 = .[illegible]1°)	5909.1[illegible]	-[illegible]1 .24	1[illegible]0°-1[illegible]°.18
C_3 (C_2C_3 = .38°)	5908.1[illegible]	-[illegible]1 .23	1[illegible]0°-[illegible]°.
C_4 (C_3C_4 = .19°)	5907.93	-[illegible]1 .24	1[illegible]0°-4[illegible]°.79
C_5 (C_4C_5 = .21°)	590[illegible].[illegible]1	-[illegible]1 .2[illegible]	1[illegible]0°-2°.21

[illegible]

ρ_1 = [illegible]000 mi $\quad e_1 = .2 \quad \omega_1 = -$ [illegible]° $\quad i_1 = 1$[illegible]°

ρ_2 = [illegible]000 mi $\quad e_2 = .2 \quad \omega_2 = -$ [illegible]°

For C_1 $\quad \beta_1 = 13°.34 \quad \beta_2$ = 1[illegible]°.2[illegible] $\quad \beta_3$ = 2[illegible]°.43 $\quad \Delta\theta$ = 1[illegible]°.[illegible]

For C_5 $\quad \beta_1 = 14°.4$[illegible] $\quad \beta_2$ = 1[illegible]°.0[illegible] $\quad \beta_3 = 239°.10 \quad \Delta\theta = 159°.$[illegible]4

(B) Quadric Approximations to the Impulse Function

General. The first quarterly progress report (SID 61-304) described a procedure for approximating surfaces of constant impulse with a quadric function in ϕ_1, ϕ_2, and ϕ_3. This approximation method was developed as part of a project to map contours of constant impulse on the IBM 740 cathode ray tube. Fig. B1 shows a set of contours obtained in the neighborhood of the optimum transfer between:

$$\rho_1 = 5000 \text{ mi}, \; e_1 = 0.2, \; \omega_1 = -30^\circ, \; i_1 = 5^\circ$$

$$\rho_2 = 6000 \text{ mi}, \; e_2 = 0.2, \; \omega_2 = +30^\circ$$

Contours are plotted for 1 ft/sec intervals in impulse, indicating the general "flatness" of the function for this particular problem. Contrast these contours with the set shown in Fig. B1 of the first quarterly report. This latter set of contours show the impulse function associated with:

$$\rho_1 = 5000 \text{ mi}, \; e_1 = 0.2, \; \omega_1 = -30^\circ, \; i_1 = 1^\circ$$

$$\rho_2 = 6000 \text{ mi}, \; e_2 = 0.2, \; \omega_2 = -30^\circ$$

Goodness of Fit. If a set of impulse surfaces is to be approximated by the quadric function $q(\Phi) = \Phi Q \Phi^T$, it is important to obtain some measure of the goodness of fit between the true and the approximating function. The usual measure employed is the RMS error over the data used to obtain the function. Investigation of this quantity for a limited number of transfer problems has led to several interesting observations about the approximation process.

The quadric function does not always provide a good approximation to the impulse surfaces. That is, for some transfer geometries the RMS error (expressed as a percentage of minimum impulse) is one or two orders of magnitude greater than for other problems. Whether or not this is characteristic of a sub-class of transfer problems has not yet been determined, although an effort is underway to investigate this possibility.

A second characteristic has been observed in connection with the approximation process. If the residuals between the quadric function and the impulse surfaces were due only to numerical "noise", one would expect a random distribution of differences over the 27 point set of values. In contrast to this expectation, there are strong indications of a systematic "ranking" in the residual values. That

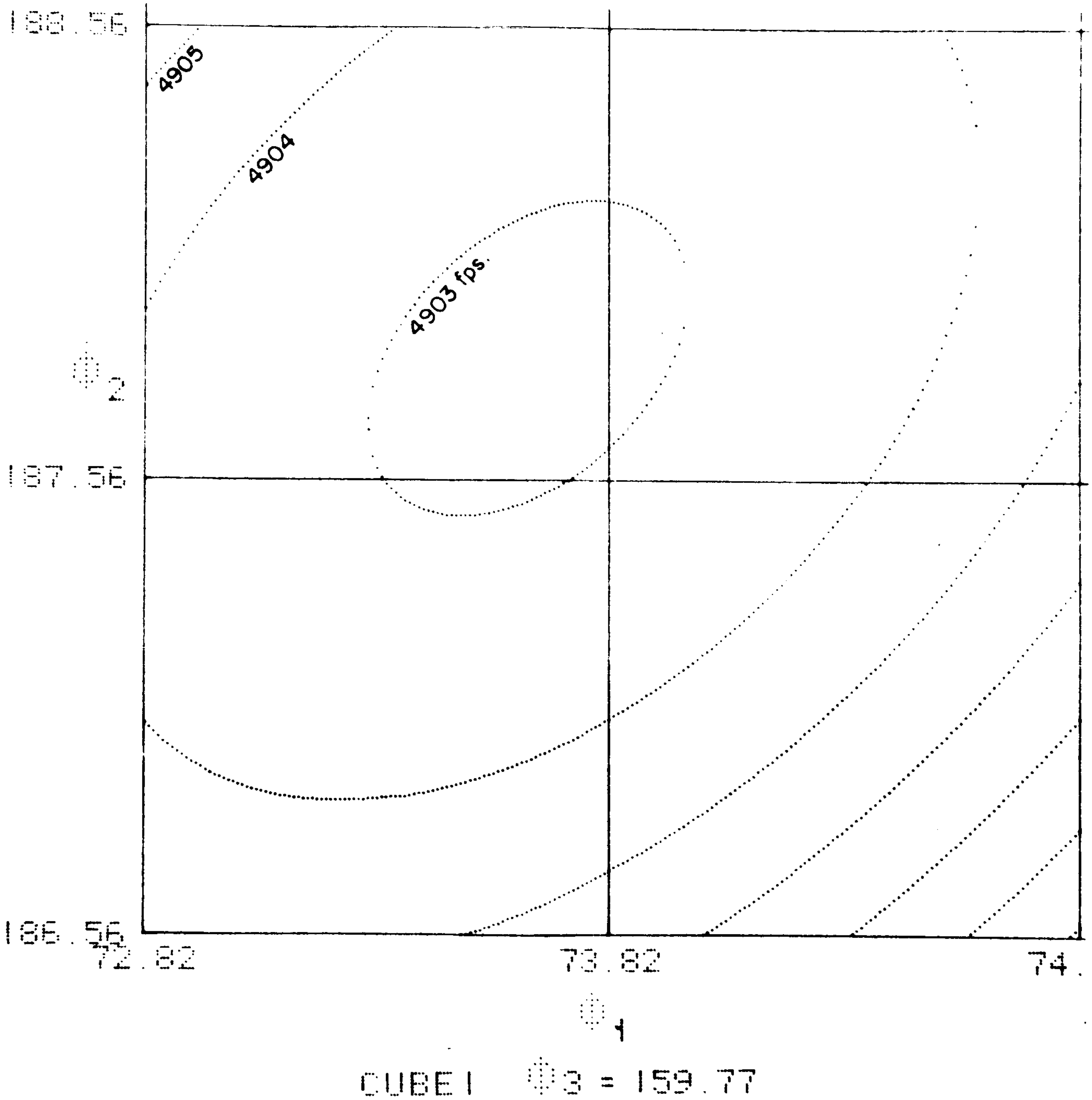

Fig. B1 (a) IMPULSE CONTOURS

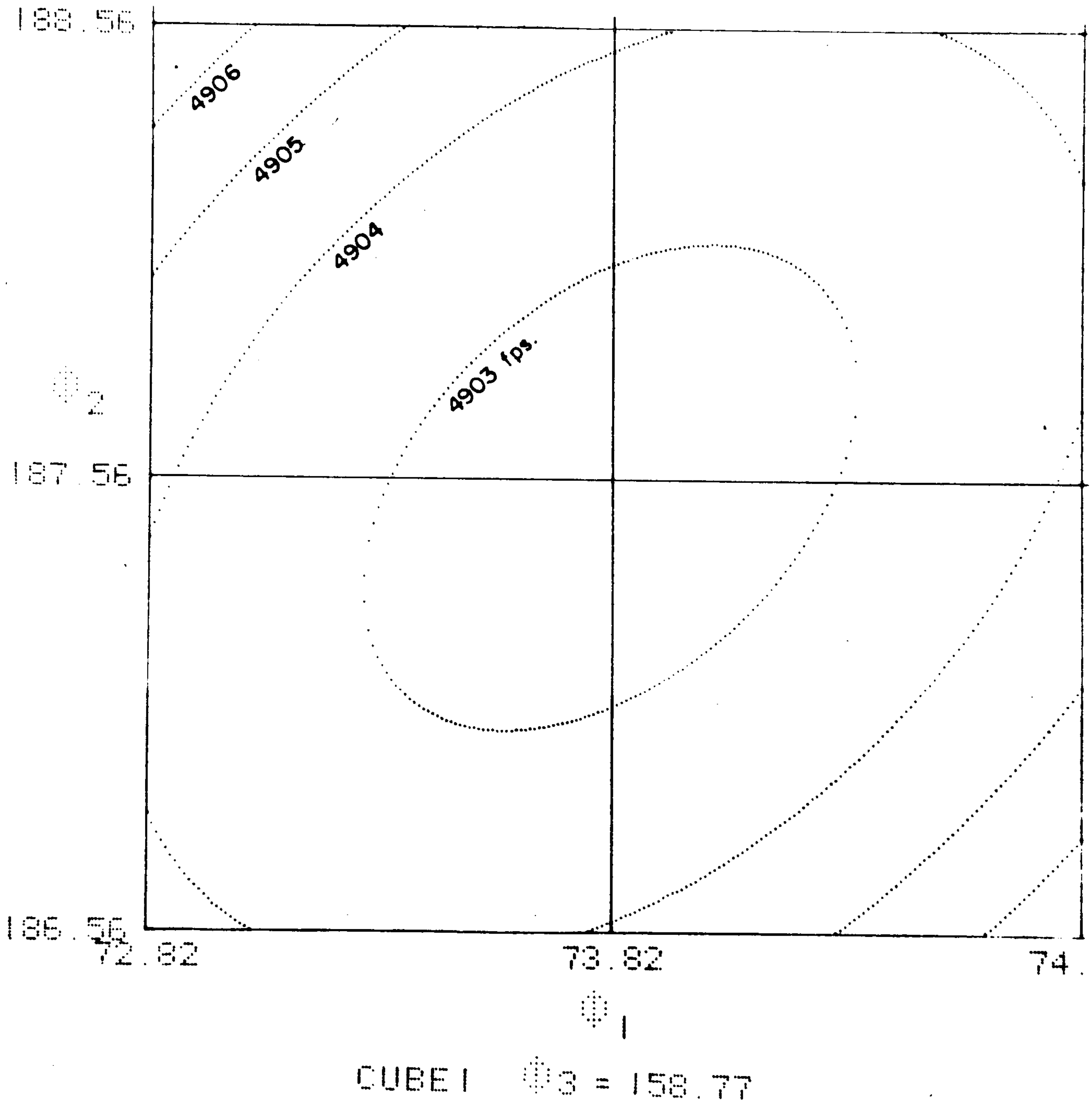

Fig. B1 (b) IMPULSE CONTOURS

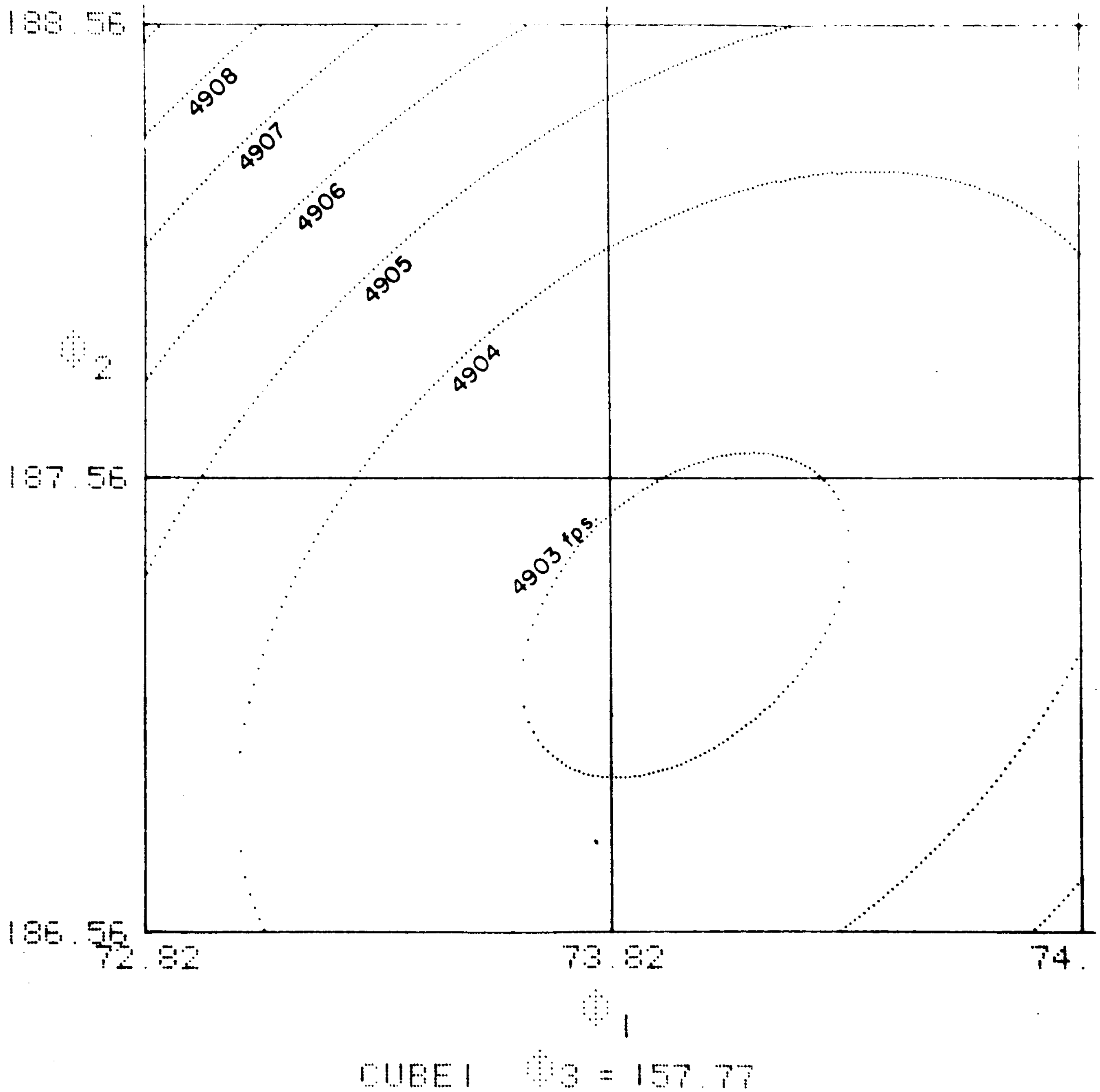

Fig. B1 (c) IMPULSE CONTOURS

is, for certain points in the generating set, the quadric approximation was systematically lower (or higher) than the true impulse function. In one experiment, the origin of the 27-point generating set, and the size of the generating cube was varied in the neighborhood of a solution. The residuals at each of the 27 points were ranked from lowest to highest and compared from case to case. The ranking was substantially the same for all cases investigated.

The Nature of the Impulse Function. Analysis of quadric approximations is leading toward an improved knowledge of the true impulse function.

The quadric surfaces exhibit certain properties which must also be properties of constant impulse surfaces within the limits of the selected approximation. Since the quadric functions are more tractable mathematically, investigation of their size, shape and orientation appears to offer an attractive avenue toward increased knowledge of the true impulse function. This in turn, should lead to further insight into the mechanism associated with optimum two impulse orbital transfers.

The following paragraphs describe the results of a very limited exploration of the approximating function. It should be emphasized that any analysis is highly speculative at this time, and that findings may be altered significantly during the next quarter.

An initial orbit with $p_1 = 5000$ and $e_1 = 0.2$ was placed at several orientations relative to a terminal orbit defined by $p_2 = 6000$, $e_2 = 0.2$ and $\omega_2 = -90^o$. An optimum transfer was determined for each case, and the impulse surfaces in the neighborhood of each minimum were approximated by a set of quadric surfaces. Each set of quadric surfaces was reduced to canonical form by an appropriate rotation and translation of coordinate axes. Apparent effects of changes in the initial orbit's inclination and argument of perigee are shown in Table B1 and Fig. B2.

Data in Table B1 describe an ellipsoidal approximation to the impulse surface with a value 10 ft/sec greater than minimum. It is interesting to note the lenticular nature of the approximating surfaces and the increased "flatness" as inclination decreases toward zero. Table B2 indicates the positions in Φ-space at which the minima occur.

Fig. B2 shows how orientation of the approximating function is affected by i_1 and ω_1. Of particular interest is the fact that changes in inclination appear as a rotation of the "natural" axes about x_1. This phenomenon will be the subject of additional experiments.

A third property of the impulse surfaces may be inferred from the

TABLE B1. CHARACTERISTICS OF THE APPROXIMATING FUNCTIONS

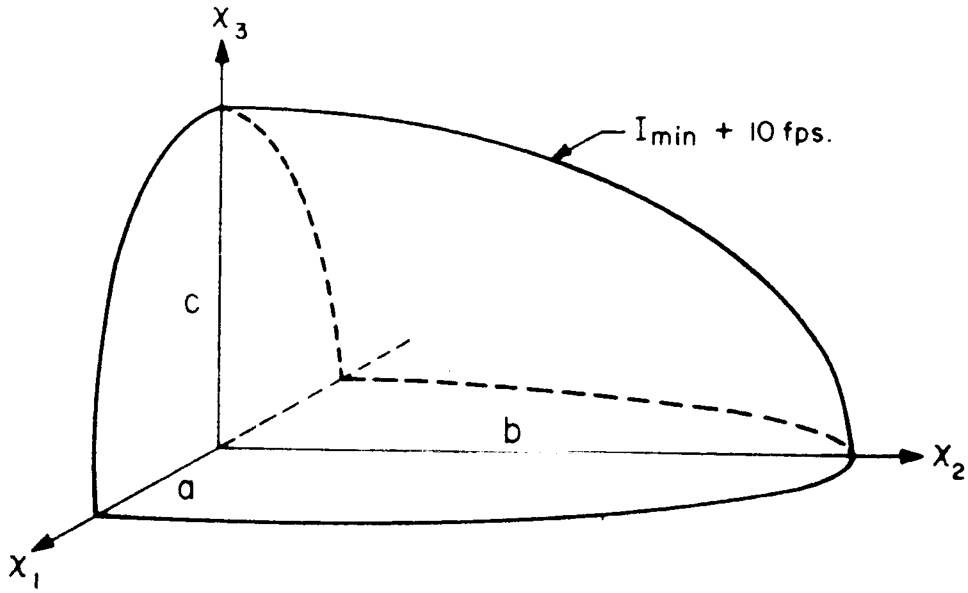

Inclination	ω_1	a	b	c	Run No.
15°	-90°	.3[illegible]°	3.72°	1.[illegible]°	QSURV 01
10°		.3[illegible]°	3.[illegible]4°	1.[illegible]°	QSURV 02
5°		.313°	4.12°	1.05°	QSURV 03
15°	-75°	.3[illegible]7°	4.[illegible]5°	1.[illegible]8°	QSURV 05
10°		.373°	4.81°	1.23°	QSURV 06
5°		.334°	4.75°	1.43°	QSURV 07

<u>Orbit Geometry</u>

p_1 = 5000 mi | p_2 = 6000 mi

e_1 = 0.2 | e_2 = 0.2

ω_1 (noted) | ω_2 = -90°

i_1 (noted)

TABLE B2. LOCATION OF OPTIMUM TRANSFERS

Inclination	ω_1	ϕ_1	ϕ_2	ϕ_3	I_{min}	RUN NO.
15°	-90°	14.55°	1[illegible]3.[illegible]°	23[illegible].14°	5[illegible].93 fps.	QSURV 01
10°		12.[illegible]4°	172.75°	23[illegible].32°	421[illegible].[illegible]4	QSURV 02
5°		10.[illegible]°	1[illegible]2.15°	23[illegible]2°	2712.[illegible]	QSURV 03
15°	-75°	16.58°	1[illegible]6.4[illegible]°	234.[illegible]°	58[illegible].05	QSURV 05
10°		14.[illegible]°	1[illegible]5.[illegible]°	234.5[illegible]°	41[illegible]0.2[illegible]	QSURV 06
5°		11.97°	175.62°	234.54°	2701.82	QSURV 0[illegible]

<u>Orbit Geometry</u>

p_1 = 5000 mi p_2 = 6000 mi

e_1 = 0.2 e_2 = 0.2

ω_1 (noted) ω_2 = -90

i_1 (noted)

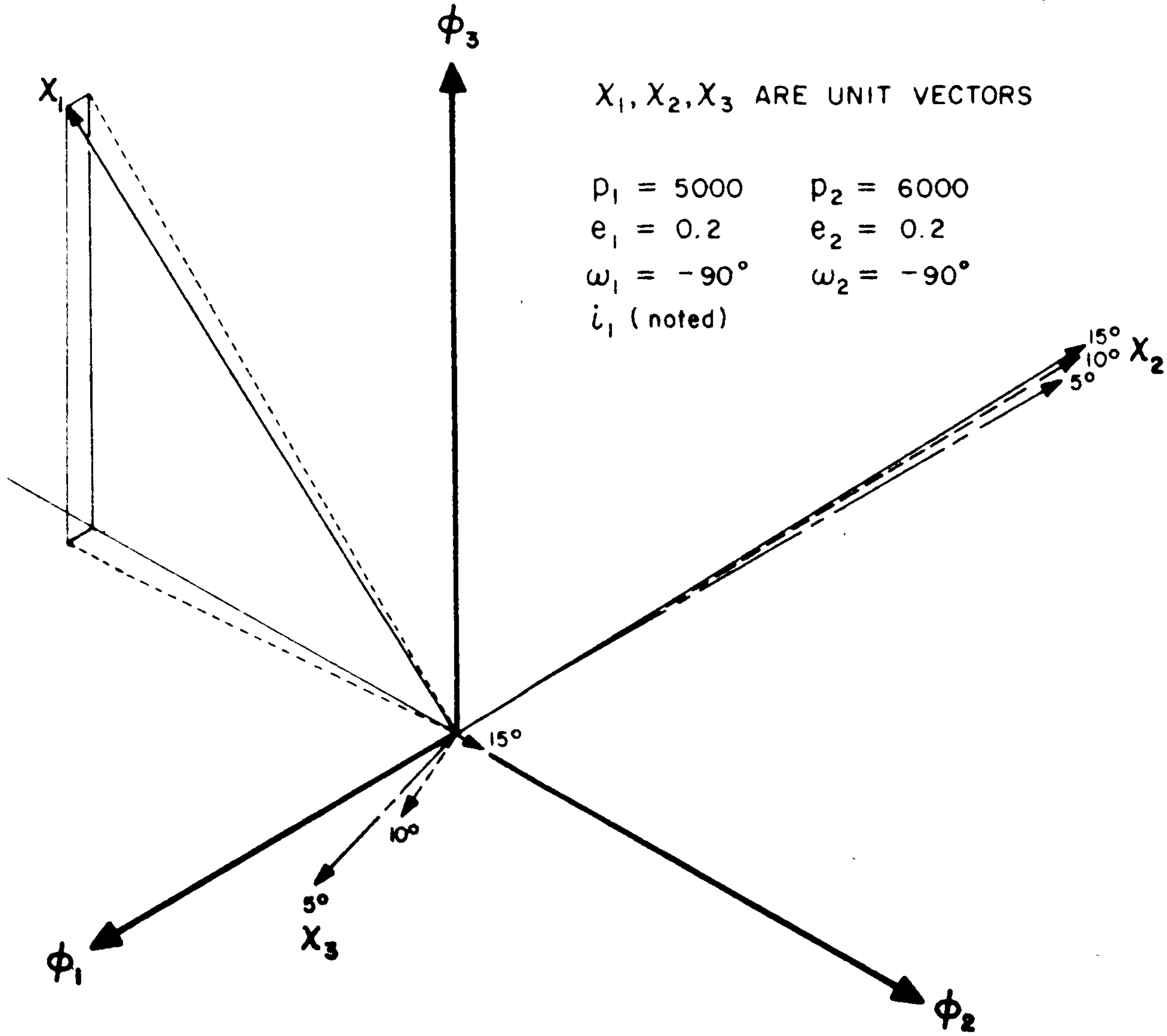

FIG. B2 ORIENTATION OF THE APPROXIMATING FUNCTIONS "ranking" phenomenon described in the previous section. From this information, it is apparent that the impulse surfaces differ in a systematic way from the approximating function. One possibility is that the surface of constant impulse is essentially ellipsoidal but that at least one of the principal axes is curved.

(C) Pictorial Representation of Transfer Geometry

It is extremely difficult to visualize the geometric relationships involved in an optimum orbital transfer without a sketch of the situation. An investigation was made into the feasibility of producing isometric or oblique drawings on a computer-controlled cathode ray plotter (the IBM 740 or Stromberg-Carlson 4020). The results of a test program are extremely encouraging with respect to both accuracy and economy. Fig. C1 shows a frame which was generated by the test problem. It required less than two seconds of 7090 time to produce.

The 4020 output consists of a 7.5 x 7.5 vellum print which is suitable for blueline reproduction, and is usually available within 3 hours of the computer run. The basic techniques should also have application to trajectory analysis, real-time display and visualization of two-variable functions. For some potential applications, machine production of these drawings should be 10 to 100 times less expensive than conventional drawing techniques. A program is now being checked out which will provide a sketch of transfer geometry as part of the optimization program output.

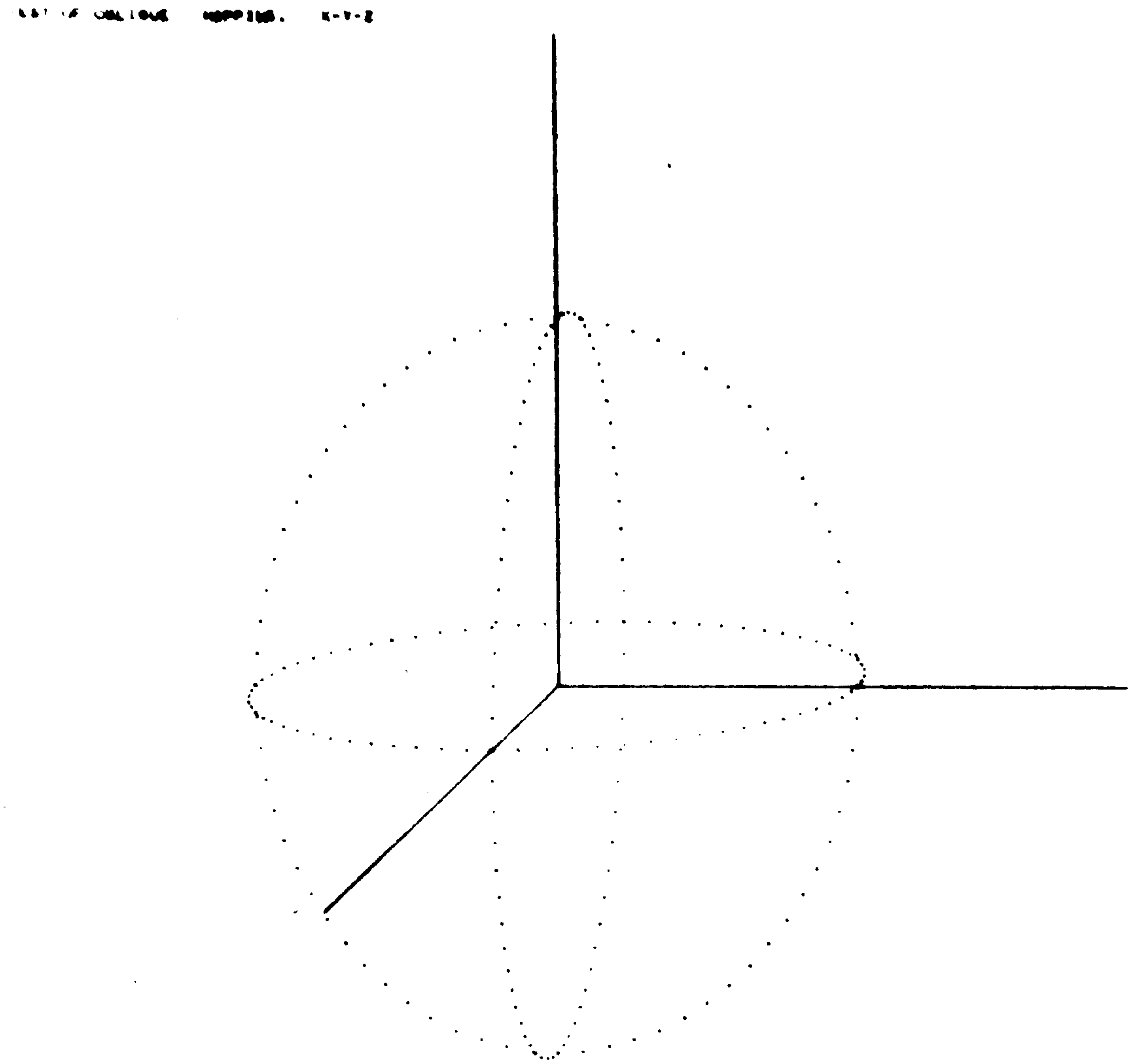

FIG. C1. TEST OF OBLIQUE MAPPING

III. PLANS FOR THE NEXT QUARTER

Mechanization of the time constrained optimization process will be completed and applied to an analysis of impulse and phase requirements for several rendezvous problems. This will lead to the consideration of the phase changing maneuver and its effect on the impulse requirements.

An effort will be made to perform a thorough exploration of representative non-coplanar transfer problems with a goal of locating, analyzing and classifying minima. Relationships between coplanar and non-coplanar cases will be developed wherever practical.

Size, shape, and orientation of the quadric approximation will be investigated further in an attempt to improve our basic knowledge of the impulse function. An improvement in the approximation as plotted can be made by making corrections to it based on an interpolation over the deviations.

Finally methods for indicating and classifying misses in rendezvous because of errors in the departure maneuver will be undertaken. This will lead to formulation of guidance and impulse accuracy requirements.

LIST OF SYMBOLS

a	semi-major axis (feet or miles)
B	binormal velocity component (ft/sec)
C	circumferential velocity component (ft/sec)
e	eccentricity
f	true anomaly
I	total impulse function (ft/sec)
I_1	impulse at departure point (ft/sec)
I_2	impulse at arrival point (ft/sec)
(i,j,k)	unit vectors in a circumferential, binormal, radial system
i	inclination
h	angular momentum per unit mass (ft^2/sec)
n	rate of change of mean anomaly (average angular velocity radians/sec)
p	semi-latus rectum (feet or miles)
Q	matrix of coefficients for $y(\Phi)$
R	radial velocity component (ft/sec)
r	radius to satellite (feet or miles)
t_1, t, t_2	time intervals on initial, transfer, and final orbits respectively
T	time of perigee crossing (seconds)
X	the vector (ϕ_1, ϕ_2, ϕ_3)
$y(\Phi)$	the quadric approximating function

LIST OF SYMBOLS (Continued)

α_1	angle between transfer orbit plane and initial orbit plane
α_2	angle between transfer orbit plane and terminal orbit plane
ζ	angle between grad I and grad τ in Φ-space
θ	angle from ascending node to position in transfer orbit
$\Delta\theta$	$\theta_2 - \theta_1$ (radians)
μ	gravitation constant (ft^3/sec^2) 1.407203×10^{16}
ρ	ratio of semi-latus recti, p_2/p_1
ϕ_1	angle from reference axis to position in initial orbit
ϕ_2	angle from reference axis to position in terminal orbit
ϕ_3	$\theta_2 - \omega$ (radians) $= f_2$
Φ	vector (ϕ_1, ϕ_2, ϕ_3, 1)
ω	argument of perigee, angle from reference axis to perigee point
τ	time difference between nodal crossings of satellite and ferry
Ω	right ascension of ascending node

Subscripts

11	on initial orbit at departure point
1	on transfer orbit at departure point(or initial orbit)
2	on transfer orbit at arrival point(or final orbit)
22	on final orbit at arrival point
3	applies to ϕ_3 only (see above)

Note: When applied to orbital elements (p, e, ω, i, Ω) subscript 1 refers to the initial orbit and subscript 2 refers to the terminal orbit. Orbital elements of transfer orbit are denoted without subscripts.